

Nucleation in bistable dynamical systems with long delay

Giovanni Giacomelli* and Francesco Marino†

CNR-Consiglio Nazionale delle Ricerche, Istituto dei Sistemi Complessi, via Madonna del Piano 10, I-50019 Sesto Fiorentino, Italy

Michael A. Zaks‡ and Serhiy Yanchuk§

Institute of Mathematics, Humboldt-University at Berlin, Rudower Chaussee 25, 12489, Berlin, Germany

(Received 16 September 2013; published 23 December 2013)

In an asymmetric bistable dynamical system with delayed feedback, one of the stable states is usually “stronger” than the other one: The system relaxes to it not only from close initial conditions, but also from oscillatory initial configurations which contain epochs of stay near both attractors. However, if the initial nucleus of the stronger phase is shorter than a certain critical value, it shrinks, and the weaker state is established instead. We observe this effect in a paradigmatic model and in an experiment based on a bistable semiconductor laser and characterize it in terms of scaling laws governing its asymptotic properties.

DOI: [10.1103/PhysRevE.88.062920](https://doi.org/10.1103/PhysRevE.88.062920)

PACS number(s): 05.45.–a, 02.30.Ks, 42.65.Sf, 89.75.Kd

I. INTRODUCTION

Traditionally, the term “nucleation” refers to the spatial effect encountered in the context of phase transitions of the first order: birth of localized buds of the new phase in the bulk of the old one. Immediate examples are crystallization in liquids cooled below the melting temperature and formation of bubbles at the transition to the gaseous phase. Typically, when the nucleus of the new phase is created inside the old one, the gain in free energy is proportional to the nucleus volume, whereas, the loss is proportional to its surface area. The balance is reached at a certain critical size of the nucleus, below which the nuclei shrink [1]. In the context of reaction-diffusion systems, nucleation occurs in bistable situations in which one of two stable regimes dominates. Here, again, survival and subsequent growth of the newborn nucleus of the dominating (below, we refer to it as “strong”) phase require that, at the moment of birth, this nucleus occupies a sufficiently large portion of available space. Since, in physical and chemical systems, phases typically fill volumes or (in the case of shallow cavities) can be characterized in terms of occupied areas, most of theoretical and experimental research on nucleation concerns two- and three-dimensional media [2,3]. In one dimension, for a large class of systems, phase transitions do not occur [1,4]. Theoretically and numerically, one-dimensional nucleation has been studied in amplitude equations [5–7] and in excitable media [8].

Here, we discuss one-dimensional nucleation which, in a seeming contrast to the above cases, occurs not in space but in time. Accordingly, a nucleus occupies not the spatial region but the time interval, and the critical size is replaced by the critical duration. This effect takes place in bistable long-delayed dynamical systems. Explicit introduction of delays into the governing equations is common in situations with finite velocities of the signal propagation, such as the dynamics in ensembles of interacting agents; it arises in a natural way, e.g.,

in problems of neuroscience [9,10] and various semiconductor laser systems (see, e.g., Ref. [11] and references therein). Quite often, in applications, the delay is long: It strongly exceeds the typical time scale of the system in the absence of delay.

For the differential equation with a delay, the initial conditions are posed on the appropriate interval. If, on the whole interval, the dependent variable takes values sufficiently close to either of the stable states (for simplicity, let the latter be time independent), that state is established as a result of the subsequent evolution. If, on the contrary, the initial interval is prepared as a sequence of alternating epochs close to different stable states, the competition starts, out of which one of them (the *strong* one) emerges as a winner. To ensure this, on the initial interval, the epoch (*nucleus*) spent near the stronger equilibrium should exceed a certain critical time: Otherwise, the too short nucleus of the strong phase shrinks, and the “weaker” state of equilibrium is established instead.

To visualize nucleation, we use the formalism, elaborated for the case of long delay in Refs. [12–16] and transform temporal dynamics into a spatiotemporal one by constructing the appropriate “pseudospace.” Below, we concentrate on the aspects related to the survival and lifetimes of nuclei, both from the theoretical and from the experimental points of view: In Sec. II, we illustrate nucleation in bistable delay systems with the help of a phenomenological scalar delay equation, and in Sec. III, we report on the experimental observation of nucleation in a laser with delayed optoelectronic feedback.

II. NUCLEATION IN THE BISTABLE DELAY DIFFERENTIAL EQUATION: A CASE STUDY

A. Dynamical system and its properties

Aiming at the description of dynamics in the bistable situation, we consider the overdamped one-dimensional motion in a double-well potential $U(x)$. The governing equation is

$$\frac{dx(t)}{dt} = -U'(x) + gx(t - \tau), \quad (1)$$

where the parameter g measures the strength of the delayed feedback. We take the simple quartic potential with $U'(x) = x(x + 1 + a)(x - 1)$ where the parameter a characterizes asymmetry in the system: When a vanishes, $U(x)$ is even.

*giovanni.giacomelli@isc.cnr.it

†francesco.marino@fi.isc.cnr.it

‡zaks@math.hu-berlin.de

§yanchuk@math.hu-berlin.de

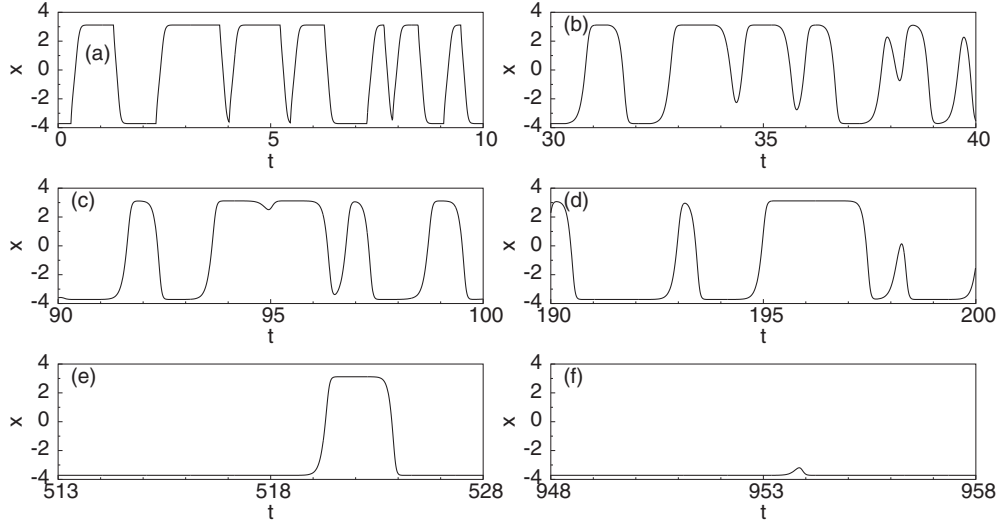


FIG. 1. Coarsening of solutions in Eq. (1) at $a = 0.5$, $g = 10$, and $\tau = 10$. Profiles of length $\tau = 10$, measured at (a) $t = 0$, (b) $t = 30$, (c) $t = 90$, (d) $t = 190$, (e) $t = 513$, and (f) $t = 948$.

Equation (1) possesses steady states at $x_0 = 0$, and $x_{\pm} = [-a \pm \sqrt{(2+a)^2 + 4g}]/2$. Below, we consider the positive feedback $g > 0$ when the latter states are stable. At $g = 0$, evolution in this system is monotonic; the larger among two characteristic time scales of relaxation to the equilibria is given by

$$\max \left\{ \frac{1}{2+a}, \frac{1}{(1+a)(2+a)} \right\}.$$

Accordingly, for $a > -0.5$, the values of delay $\tau > 10$ can be viewed as large.

For numerical integration of Eq. (1), we have used the original algorithm of the recurrent Taylor expansion of the 30th order with a constant time step. As an initial profile for integration, we take a nonmonotonic sequence $x(t)$ in which the maxima (minima) lie, respectively, in the range of positive (negative) values of x . The exact shape of the initial profile seems to be of little significance: The oscillations very soon become nearly rectangular with alternating plateaus near the steady states x_{\pm} , separated by short ascending and descending segments. Here, the process of *coarsening* takes place: Under positive values of a , the plateaus at x_{-} become longer, whereas, their counterparts at x_{+} gradually shrink, until finally, the oscillations cease, and the steady state x_{-} is established. Different stages of this process are presented in Fig. 1. At negative values of a , the same effect takes place, but the eventual winner is now state x_{+} .

B. Spatiotemporal patterns. Coarsening

At a closer look, temporal evolution of the system appears to unfold in two characteristic time scales: nearly stationary intervals which can last almost up to τ alternate with segments of rapid changes with duration on the order of $1/g$. By taking an appropriate small number δ ($0 < \delta \sim 1/g \ll \tau$) and cutting the sufficiently long trajectory $x(t)$ into the segments (frames) of length $\tau + \delta$, it is possible to ensure that the profile in each subsequent frame is nearly the same as in the preceding

one. On the much slower time scale, the profile inside the frame gets deformed: The coarsening takes place. Notably, the value of δ varies when the parameters a and/or g are varied, but it is almost insensitive to variation in delay depth τ . By separating the time scales, we put the purely temporal process of coarsening into the artificial pseudospace and obtain a convenient visualization. The spatiotemporal representation is constructed by decomposition of every positive value t of time into $t = n(\tau + \delta) + \sigma$ with natural n and real σ ($0 \leq \sigma < \tau + \delta$). The values of σ and n —respectively, number of the frame and position *inside* the frame—play the roles of the spatial and temporal coordinates. This construction is based on the well-established analogy between the systems with long-delay and spatially extended one-dimensional systems [12–16].

The corresponding visualization of coarsening is presented in Fig. 2. In these coordinates, the transitions between the steady states look like propagating ascending and descending fronts: In the process of coarsening, the fronts coalesce pairwise and disappear so that, ultimately, only one state remains. In general, the outcome depends on the balance of the front velocities: If the ascending front propagates faster than its descending counterpart, state x_{+} eventually disappears; in the opposite case, x_{-} is the weaker phase. Duration of the coarsening process is inversely proportional to the difference in the front velocities [17]. The degenerate situation in which velocities of both fronts coincide will be referred to as *balanced*; in Eq. (1), it corresponds to the symmetric potential at $a = 0$.

Typically, an initial segment of the stronger phase [green (dark) in the color box of Fig. 2] expands at the cost of the weaker phase [respectively, yellow (bright)]. We observe, however, that, in the initial profile, there are several small pieces of the stronger phase which fail to grow and eventually subside. Magnification of one such piece in the right panel indicates that there is a critical size (duration) for the nucleus of the strong phase. A nucleus of a subcritical duration (central dark stripe) is suppressed by the weaker phase. In contrast, a

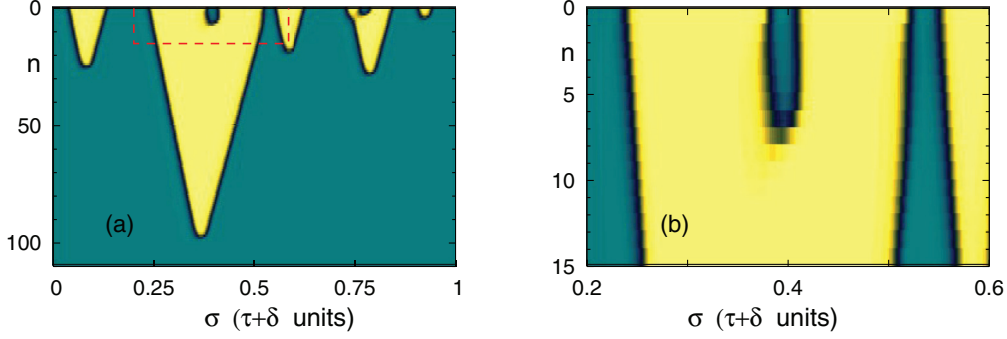


FIG. 2. (Color online) Coarsening in pseudospace of Eq. (1). Same parameter values as in Fig. 1. Vicinity of x_- (strong phase) is painted green (dark); vicinity of x_+ (weaker phase) is painted yellow (bright). (a) Propagation of fronts. (b) Magnification of the segment [delineated in (a) by the dashed line] near the nucleus of the strong phase.

nucleus with duration slightly bigger than the critical one (the right dark stripe), after a certain transient process, starts to expand.

Numerical results confirm that, for $\tau \geq 5$, the size of the critical nucleus t_{crit} is determined by the employed values of g and a but practically (to the accuracy of 10^{-15}) does not depend on the value of delay τ [18].

C. Lifetime of a nucleus

Before the final settling to one of the steady states, the trajectory oscillates back and forth between x_+ and x_- , hence, it seems natural to characterize the lifetime for the subcritical nucleus by the moment of the last zero crossing. Numerical data, presented in the left panel of Fig. 3, demonstrate that the lifetime depends monotonically on the deficit of size: The shorter the original nucleus, the faster it decays. A closer look at these data allows us to discern two different asymptotic dependencies and, thereby, to distinguish between the slightly subcritical nuclei and those whose length (duration) is distinctly below the critical size.

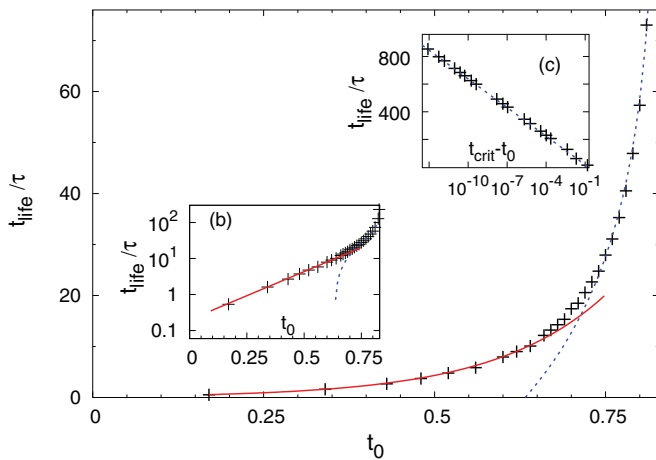


FIG. 3. (Color online) Dependence of the lifetime of the subcritical nucleus on its initial size t_0 for Eq. (1) at $a = 0.04$, $g = 5$, and $\tau = 5$. Pluses: last zero crossings (numerics). Solid line: exponential dependence. Dashed curve: logarithmic law (6). Inset (b): exponential growth at small t_0 . Inset (c): logarithmic asymptotics near the critical nucleus.

Even for relatively short nuclei, their original lengths are much larger than the widths of the fronts on their borders. This allows us to characterize the motion of fronts by utilizing the formalism, developed in Ref. [19] for the dynamics of weakly interacting kinks in evolution equations without delay. Formally treating the discrete pseudotime n as a continuous independent variable, we phenomenologically describe the time-dependent size $W(n)$ of the nucleus by the equation,

$$\frac{dW}{dn} = -Be^{-\beta W} + A, \quad (2)$$

with positive coefficients β , A , and B ($A < B$) where the first term describes the exponentially weak attraction between the distant fronts and the constant term is the difference between the propagation velocities of the solitary ascending and descending fronts. In the balanced situation [recall that, in Eq. (1), it corresponds to $a = 0$], the latter term vanishes. By rescaling the units of W and of pseudotime n , the parameter dependence is restricted to the combination $A/(\beta B)$, which, close to the balance, is approximately proportional to a in Eq. (1).

According to Eq. (2), there exists a critical initial duration $W_c = \ln(B/A)/\beta$: The nuclei with initial duration $W_0 < W_c$ decrease and vanish within the finite time, whereas, the ones with $W_0 > W_c$ grow unboundedly. The latter case describes coarsening; the velocity with which the nucleus of the strong phase broadens tends to A . In contrast, nuclei with subcritical initial length shrink. Their lifetimes are

$$n_{\text{life}} = \frac{1}{A\beta} \ln \frac{B - A}{B - A \exp(\beta W_0)}. \quad (3)$$

For a short (but not too short: $\beta W_0 \gg 1$) initial nucleus in a nearly balanced configuration, this is reduced to the exponential dependence,

$$n_{\text{life}} \approx \frac{\exp(\beta W_0)}{B\beta}. \quad (4)$$

In contrast, for slightly subcritical nuclei whose initial durations are close to W_c , the asymptotic logarithmic law,

$$n_{\text{life}} \approx -\frac{1}{A\beta} \ln(W_c - W_0) \quad (5)$$

should hold.

Results of numerical integration of Eq. (1), summarized in Fig. 3, are in good accordance with the above theoretical predictions. In the left inset of Fig. 3, for sufficiently small nuclei, the exponential dependence of lifetime on the initial duration t_0 is well identifiable. Growth of the initial duration leads, after the crossover interval, into the domain close to the threshold t_{crit} in which another asymptotic law takes place. In appropriate coordinates used in the right inset of Fig. 3, we observe that the number of delays during which a nucleus persists, obeys a logarithmic dependence of the type (5),

$$\frac{t_{\text{life}}}{\tau} \approx -\kappa \ln(t_{\text{crit}} - t_0). \quad (6)$$

Estimates from the dynamics of Eq. (1) at different parameter values show that slope κ varies with the asymmetry a of the system but is practically independent of τ (Fig. 4).

Dynamically, the critical nucleus can be viewed as an unstable periodic solution of Eq. (1) with period $\tau + \delta$ and a single Floquet multiplier outside the unit circle. The stable manifold of this solution has codimension 1 and serves in the phase space as part of the boundary between the attraction basins of two fixed points which correspond to the strong and the weak phases, respectively. A trajectory which starts from a slightly subcritical nucleus approaches this periodic solution along its stable manifold, stays in its vicinity for a certain time, and finally, departs to the equilibrium which corresponds to the weak phase. A slightly supercritical nucleus approaches the unstable periodic state as well; its subsequent evolution, in contrast, leads to growth of the nucleus and

ends up in the establishment of the strong phase. The overall time spent in the vicinity of the unstable periodic solution constitutes nearly the whole (save for the very beginning and the short final stage) lifetime of a subcritical nucleus, therefore, its duration is governed by the largest Floquet multiplier μ , responsible for the instability. In each next frame, compared to the previous one, the distance from the stable manifold is approximately multiplied by μ , until a certain finite distance is reached, beyond which the unstable periodic solution becomes irrelevant for dynamics, and linear relaxation to the steady state (see the next subsection) begins. Hence, slope κ , as introduced in Eq. (6), is related to μ as

$$\kappa = \frac{1}{\ln \mu} \longleftrightarrow \mu = \exp(1/\kappa). \quad (7)$$

The conjecture about the inter-relation between the nucleation and the unstable periodic solution has been confirmed by independent numerical analysis of the unstable periodic orbit in Eq. (1), performed with the help of the bifurcation software package DDE-BIFTOOL [20]. A search for different values of a , g , and τ has detected the family of unstable periodic orbits whose unstable manifold has codimension 1. Under fixed moderate values of a and g , the largest Floquet multiplier of this orbit is almost τ independent: For $\tau \geq 5$, its first six decimal digits do not change. Comparison of the values of this multiplier with estimates (7) obtained from the fitting data of lifetimes of the nuclei displays a remarkable coincidence within 1%. This strengthens our view upon nucleus dynamics as a passage close to the unstable periodic state.

At positive values of the delay feedback g , Eq. (1) is a monotone dynamical system and, hence, cannot possess stable periodic solutions [21]. However, in the case of vanishing asymmetry $a = 0$, the relevant periodic state can be made nearly marginal (for example, at $g = 2$ and $\tau = 5$, $\mu < 1.01$, which results in the strong increase in slope κ and noticeably prolongs the life of slightly subcritical nuclei.

D. Final relaxation

Presented results bear an obvious resemblance to reaction-diffusion phenomena. In one aspect, however, there is a distinction: This concerns propagation of the nucleus at its final stage during linear relaxation to the steady state. There, the description with the help of Eq. (2) is not valid: The boundaries of the nucleus at that stage are neither sharp fronts nor distant.

Linearizing the equations near the (weak) stable steady state, we obtain

$$\phi_n'(\sigma) = \eta \phi_n(\sigma) + g \phi_{n-1}(\sigma), \quad (8)$$

where a prime denotes differentiation with respect to the pseudospacial coordinate σ and ϕ_n is the profile, which is localized within the n th frame and vanishes on both of its borders. Since the steady state is stable, the value of η is negative. The feedback strength g , in contrast, is positive. A substitution $\phi_k = e^{\eta \sigma} \xi_k$ results in

$$\xi_n' = g \xi_{n-1},$$

hence, starting from a non-negative ϕ_0 , the functions $\phi_j(\sigma)$ keep staying non-negative for all j . We interpret ϕ_n as the

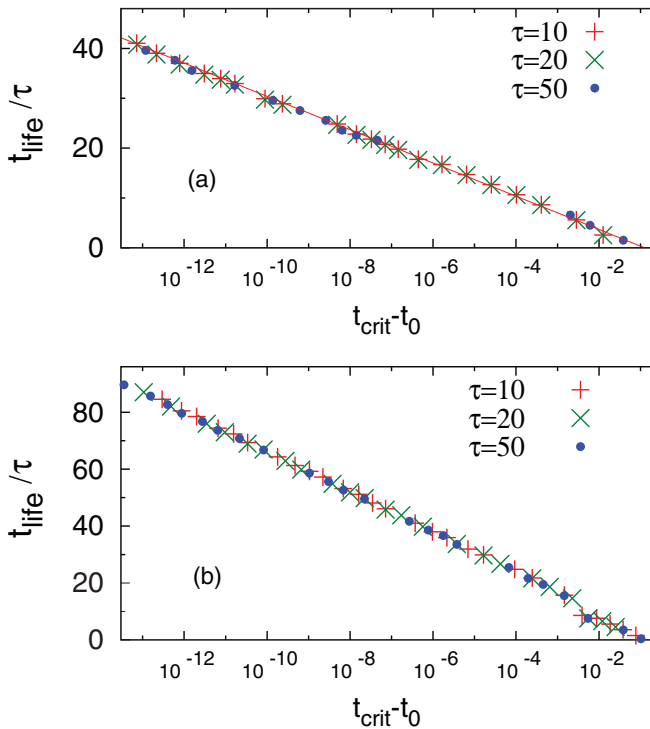


FIG. 4. (Color online) Lifetime of subcritical nuclei for Eq. (1) at $g = 10$ and different values of delay τ . t_{crit} : critical size of the nucleus; t_0 : size of the nucleus in the initial profile. (a) $a = 1$, nucleus of x_- ($t_{\text{crit}} = 0.168864$), $\kappa \approx 1.45$; (b) $a = -1/2$, nucleus of x_+ ($t_{\text{crit}} = 0.233400$), $\kappa \approx 3.05$.

family of distributions and consider their moments,

$$M_n^{(k)} = \int \phi_n(\sigma) \sigma^k d\sigma, \quad (9)$$

where integration is performed over the whole n th frame. Since ϕ_n vanishes identically on the frame borders, integration by parts yields

$$kM_n^{(k-1)} + \eta M_n^{(k)} + gM_{n-1}^{(k)} = 0. \quad (10)$$

Dividing these values by $M_n^{(0)} = (-g/\eta)^n$, we arrive at the recurrences for normalized moments $N_n^{(k)} = M_n^{(k)}/M_n^{(0)}$,

$$kN_n^{(k-1)} + \eta N_n^{(k)} = \eta N_{n-1}^{(k)}. \quad (11)$$

Remarkably, normalized moments are independent of the feedback strength g . For the first moment of the distributions, (11) results in

$$N_n^{(1)} = N_{n-1}^{(1)} - 1/\eta = \dots = N_0^{(1)} - n/\eta, \quad (12)$$

i.e., in every next frame, the center of mass of the nucleus is shifted to the right with respect to the previous frame by the value of $1/|\eta|$: The mean value of the solution drifts with the velocity $-1/\eta$.

The second normalized moment obeys

$$N_n^{(2)} = N_{n-1}^{(2)} - \frac{2}{\eta} N_n^{(1)} = \dots = N_0^{(2)} - \frac{2n}{\eta} N_0^{(1)} + \frac{n(n+1)}{\eta^2}. \quad (13)$$

Hence, the variance $\text{Var}_n = N_n^{(2)} - (N_n^{(1)})^2$ increases linearly with a rate $1/\eta^2$,

$$\text{Var}_n = \text{Var}_0 + n/\eta^2, \quad (14)$$

i.e., in each next frame, the distribution is broader. To summarize, while proceeding from one frame to the next one, the decaying nucleus becomes less sharp and drifts to the right. The drift velocity only depends on the linearization near the weak state, is independent of the feedback strength g , and in general, differs from the velocities of ascending and descending fronts during the nonlinear stage of the nucleus evolution (the latter are close to $1/g$ [17]). Therefore, in the reference frame in which the bulk of the nucleus does not move, the very ‘‘tip’’ of the decaying part becomes skewed. This is a clear deviation from the usual properties of reaction-diffusion in isotropic media where the spatial symmetry of the pulse is maintained until its complete absorption.

III. NUCLEATION: EXPERIMENT IN A BISTABLE LASER WITH LONG-DELAYED FEEDBACK

Recently, we have provided evidence of reaction-diffusion-type dynamics in a bistable laser with long-delayed feedback with front creation, propagation, and annihilation leading to coarsening [17]. Here, we use the same experimental setup, but the focus is placed onto the nucleation-related aspects.

The system is based on a vertical cavity laser in a regime of bistable emission onto two linear orthogonal polarizations of the optical field. The polarized laser emission is detected, and the signal is delayed by means of an acquisition board and a suitable real-time software, which possibly allows very long

delays. The delayed output is then summed back with the bias to the pump current of the laser.

Depending on the control parameters, the delayed system displays two stable states. A jump between them, which can be induced either by noise or by a choice of the initial state, may propagate in the (pseudo) space. The switching time is bandwidth limited at a few microseconds and represents the typical (and fastest) time scale of the system. In the measurements reported here, the delay time was set at different values, usually longer than 19 ms (see the figure caption). Hence, we are in the long-delay regime with an aspect ratio exceeding 10^2 [12–15]; in this case, we did not observe any influence of the delay time value on the observations.

In the measurements, opposite fronts (e.g., jumps connecting lower to higher and higher to lower intensity values) annihilate when colliding, eventually leading to a homogeneous (*strong*) state [17].

As suggested by analysis of the model (1), we expect formation of nuclei in the strong phase for a proper choice of the parameters and initial conditions. To this aim, by setting the laser pump current and the coupling of the feedback loop, we choose a regime in which a coarsening process takes place. In this case, the strong phase (shown by white in the figures) corresponds to the higher laser intensity. Here, preparing the initial state as a random sequence of the two stable states, the propagation of the fronts would gradually lead the system to relax to the strong state through coarsening as shown in Fig. 5.

In this case, analyzing the (pseudo-) temporal behavior of a random intensity pattern, formation of buds of the strong phase is observed within islands of the weak phase (see the inset of Fig. 5). Such structures have finite lifetimes depending on their initial sizes (i.e., duration in the pseudospace).

To shed light on the dependence of the nuclei lifetimes on their initial sizes, we perform a measurement by setting, as the

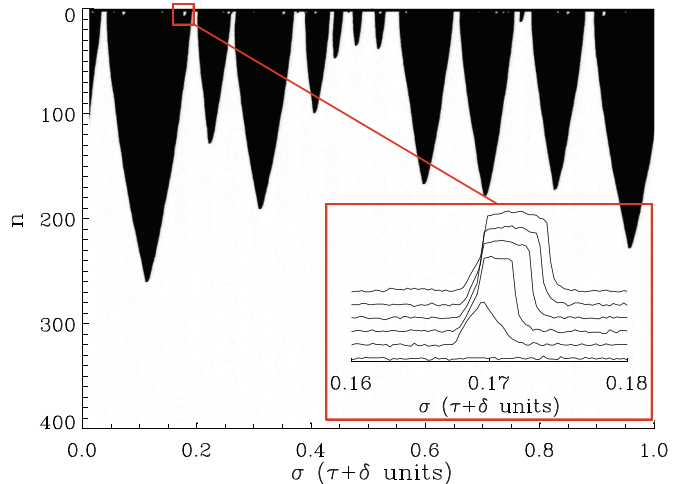


FIG. 5. (Color online) Experiment. Spatiotemporal representation of the bistable laser intensity; black (respectively, white) represents the lower (respectively, higher) intensity stable state. The initial state is a random sequence of the two stable amplitudes on the first delay interval (here, set to 19 ms). Coarsening is observed as the motion and annihilation of fronts between the states and the eventual onset of the homogeneous (*strong*) state. Formation of nuclei of the strong phase is observed (inset).

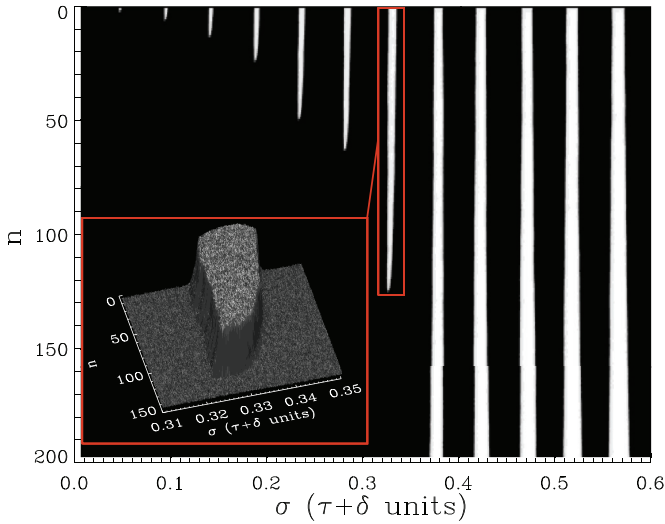


FIG. 6. (Color online) Experiment. The initial state (in a delay unit of 19 ms) is prepared as a comb of pulses with linearly increasing (from left to right) width in the strong phase. A zoom of the full pattern is presented. Nucleation is observed as a finite lifetime of the pulses for widths up to a critical value, beyond which the coarsening process takes place. Final relaxation towards the weak phase occurs with a different velocity (inset).

initial condition, a comb of pulses with (linearly) increasing widths, corresponding to increasing durations in the strong phase. The pulses are sufficiently separated in the pseudospace to let them be considered as independent. In this way, a single measurement allows us to test the effect of the different sizes of the pulses in the same experimental conditions.

As shown in Fig. 6, the choice of a different width for the initial pulse can drastically change the way it propagates and survives or not in the coarsening process. More precisely, it is observed that, for small widths, the pulse propagates and then disappears due to the annihilation of the two fronts which delineate it (Fig. 6, leftmost pulses). Notably, the velocity of the pulse in the final part of the process appears systematically different from the propagation velocity as predicted in the analysis of Sec. II D.

We remark that, in such a case, annihilation takes place even if the state between the fronts is the strong phase.

As the initial width is increased, the duration (in the pseudotime) of the pulses increases as well, until the threshold value is reached, beyond which the pulses do not disappear but expand with time (Fig. 6, rightmost pulses) as expected in the coarsening regime.

To quantify the observed behavior, we analyze the time dependence of the area of the pulse, i.e., the spatial integral over the pulse profile. Such an indicator is roughly proportional to the pulse width and allows for a substantial reduction in the undesired signal fluctuations.

The results are shown in Fig. 7 where we plot the temporal behavior of the pulse area P . For a given (small) width, relaxation of P towards zero is observed with a slow initial part whose duration increases strongly with the width duration. The final part of the relaxation, instead, is apparently triggered by the crossing of a well-defined threshold and follows a shape which is independent of the initial width (see the inset of

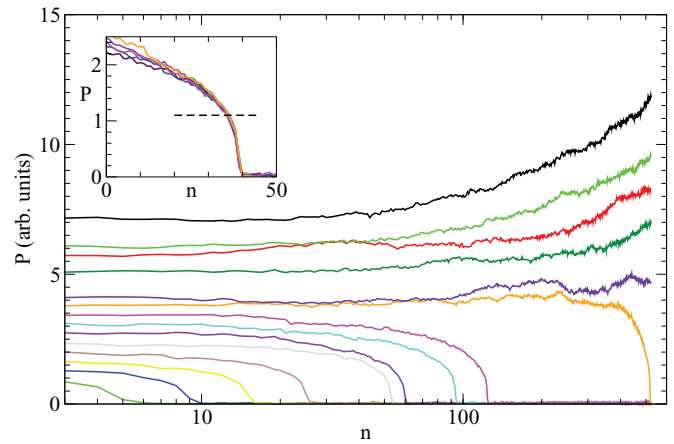


FIG. 7. (Color online) Experiment. Temporal behavior of the pulse area for linearly increasing pulse widths (curves from bottom to top). Inset: nuclei final relaxation; the curves are shifted in time to overlap. The horizontal dashed line in the inset marks the crossing point and is used to evaluate the nucleus lifetime (see the text). The delay time is 57 ms.

Fig. 7). For widths higher than the critical value, the pulse eventually broadens, and the area (linearly) diverges in time in accordance with the coarsening process.

A comparison of experimental results with the predicted scaling (4) of the nucleus lifetime with its width (or area) has been carried out as well. In Fig. 8, we plot the variable $\exp(P)$ for different nuclei. In this case, linear scaling is expected, and it is, indeed, observed for a large range of time intervals, thus, confirming the exponential character of the dependence between the small original width of the nuclei and their lifetimes.

Increasing the nucleus width and approaching the critical size W_c , different scaling is expected [see Eq. (5)]. On the other hand, from the experimental point of view, already, the exponential dependence of the nuclei lifetimes from their widths sets a strong limitation on the measurements. In particular, the fluctuations in the trajectories (as seen, e.g.,

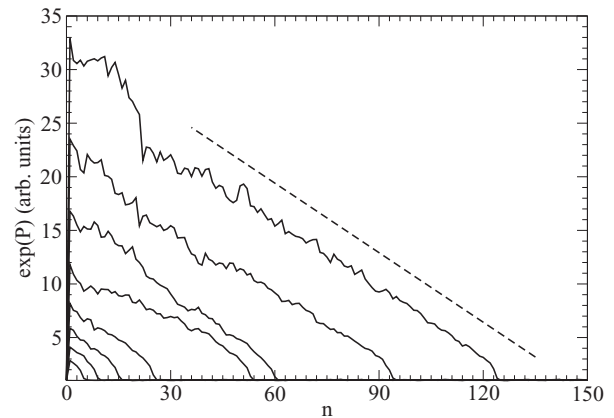


FIG. 8. Experiment. Temporal behavior of the nucleus area for linearly increasing widths (curves from bottom to top). The dashed line represents exponential scaling as predicted by Eq. (4). The delay time is 57 ms.

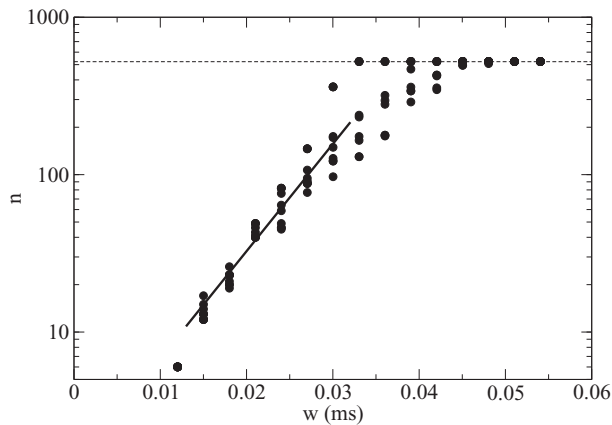


FIG. 9. Experiment. Lifetime of an ensemble of pulses as a function of their initial widths. The duration is evaluated at the crossing point (depicted in the inset of Fig. 7) in the case of a nucleus relaxing to zero and set to the limit of the measurement window (horizontal dashed line) otherwise. Several runs are carried out for the same initial width. The full line indicates an exponential increase. The delay time is 57 ms.

in Fig. 7) are possibly due to the effect of noise on the position of the fronts.

To partially overcome the problem, the measurement of the pulse lifetime would better be carried out as a statistical average over many different realizations. In Fig. 9, we report the result of several runs, plotting the lifetimes of the nuclei (evaluated as the time needed to reach the crossing point, see the inset of Fig. 7) for increasing widths.

In this case, however, only the first exponential increase is observed for small widths, then the limited measurement window (depicted by the horizontal dotted line) imposed by the stability of the experimental system prevents us from quantitatively characterizing the behavior for larger widths below the critical value W_c . We remark, however, that an increase in the spreading of the measurements (described, e.g., by the standard deviation) is clearly evident, and it

is compatible with possible deviations from the exponential behavior measured for small widths.

IV. SUMMARY AND CONCLUSIONS

It is becoming increasingly evident that many crucial effects in purely temporal systems with long delays are related to their hidden spatiotemporal properties. These properties are instrumental in generating such pattern-forming effects as coarsening [17], Eckhaus instability [16], or chimera states [22] in delay systems. Here, we have presented our observations of another typical spatiotemporal phenomenon—nucleation—in the delay setting. In a phenomenological model, we have characterized scaling of the nucleus duration with its initial size, both for the close-to-zero and for the close-to-critical situations. Numerically observed behavior discloses both analogies to and distinctions from dynamics of nucleus fronts in a conventional one-dimensional reaction-diffusion system.

Experimental observation of this effect has also been performed in a setup with a bistable vertical cavity laser with long-delayed optoelectronic feedback. Formation and propagation of nuclei have been observed, and their lifetimes have been studied by a suitable preparation of the initial state (a delay unit) of the laser. The observed scaling of the nucleus lifetime follows the theory for small initial size. The limitation imposed by the system stability and the exponential sensitivity of the lifetime to fluctuations of the front position prevented us from characterizing the scaling for larger initial nuclei (closer to the critical size). However, the spread in the measurements is compatible with the predicted scaling. A more detailed study of close-to-critical regimes could be handled by several realizations (as described and demonstrated here) and is planned for a future study.

ACKNOWLEDGMENTS

We acknowledge the German Research Foundation (DFG) for financial support in the framework of the Collaborative Research Center SFB 910 (S.Y. and G.G.) and Research Center MATHEON (M.A.Z.).

-
- [1] L. D. Landau and E. M. Lifshitz, *Theoretical Physics*, 3rd. ed. (Elsevier-Butterworth-Heinemann, Oxford, 2005), Vol. 5.
 - [2] M. Bär, C. Zülicke, M. Eiswirth, and G. Ertl, *J. Chem. Phys.* **96**, 8595 (1992).
 - [3] D. Gomila, P. Colet, G.-L. Oppo, and M. San Miguel, *J. Opt. B: Quantum Semiclassical Opt.* **6**, S265 (2004).
 - [4] J. A. Cuesta and A. Sánchez, *J. Stat. Phys.* **115**, 869 (2004).
 - [5] M. Argentina and P. Coulet, *Phys. Rev. E* **56**, R2359 (1997).
 - [6] M. van Hecke and M. Howard, *Phys. Rev. Lett.* **86**, 2018 (2001).
 - [7] I. S. Aranson and L. Kramer, *Rev. Mod. Phys.* **74**, 99 (2002).
 - [8] M. Argentina, P. Coulet, and L. Mahadevan, *Phys. Rev. Lett.* **79**, 2803 (1997).
 - [9] B. Bard Ermentrout and D. H. Terman, *Mathematical Foundations of Neuroscience* (Springer, New York, 2010).
 - [10] E. Izhikevich, *Neural Comput.* **18**, 245 (2006).
 - [11] M. C. Soriano, J. Garcia-Ojalvo, C. R. Mirasso, and I. Fischer, *Rev. Mod. Phys.* **85**, 421 (2013).
 - [12] F. T. Arecchi, G. Giacomelli, A. Lapucci, and R. Meucci, *Phys. Rev. A* **45**, R4225 (1992).
 - [13] G. Giacomelli, R. Meucci, A. Politi, and F. T. Arecchi, *Phys. Rev. Lett.* **73**, 1099 (1994).
 - [14] G. Giacomelli and A. Politi, *Phys. Rev. Lett.* **76**, 2686 (1996).
 - [15] G. Giacomelli and A. Politi, *Physica D* **117**, 26 (1998).
 - [16] M. Wolfrum and S. Yanchuk, *Phys. Rev. Lett.* **96**, 220201 (2006).
 - [17] G. Giacomelli, F. Marino, M. A. Zaks, and S. Yanchuk, *Europhys. Lett.* **99**, 58005 (2012).
 - [18] The critical value itself depends, of course, on the configuration of the initial profile; we studied the dependencies in families

of profiles where the initial nucleus size t_0 could be varied continuously.

- [19] K. Kawasaki and T. Ohta, [Physica A](#) **116**, 573 (1982).
- [20] K. Engelborghs, T. Luzyanina, D. Roose, [ACM Trans. Math. Software](#) **28**, 1 (2002).
- [21] H. L. Smith, *Monotone Dynamical Systems: An Introduction to the Theory of Competitive and Cooperative Systems*, Mathematical Surveys and Monographs Vol. 41 (AMS, Providence, 1995).
- [22] L. Larger, B. Penkovsky, and Y. Maistrenko, [Phys. Rev. Lett.](#) **111**, 054103 (2013).